Published in final edited form as:
Vet Immunol Immunopathol. 2015 February 15; 163(0): 134–145. doi:10.1016/j.vetimm.2014.11.013.

Isolation, Characterization, and Functional Analysis of Ferret Lymphatic Endothelial Cells

Stella J. Berendam[1], **Beth A. Fallert-Junecko**[1], **Michael A. Murphy-Corb**[2], **Deborah H. Fuller**[3], and **Todd A. Reinhart**[1]

[1]Department of Infectious Disease and Microbiology, Graduate School of Public Health, University of Pittsburgh, Pittsburgh, PA 15261, USA.

[2]Department of Microbiology and Molecular Genetics, School of Medicine, University of Pittsburgh, Pittsburgh, PA 15261, USA.

[3]Department of Microbiology, School of Medicine, University of Washington, Seattle, WA 98195, USA.

Abstract

The lymphatic endothelium (LE) serves as a conduit for transport of immune cells and soluble antigens from peripheral tissues to draining lymph nodes (LNs), contributing to development of host immune responses and possibly dissemination of microbes. Lymphatic endothelial cells (LECs) are major constituents of the lymphatic endothelium. These specialized cells could play important roles in initiation of host innate immune responses through sensing of pathogen-associated molecular patterns (PAMPs) by pattern recognition receptors (PRRs), including toll-like receptors (TLRs). LECs secrete pro-inflammatory cytokines and chemokines to create local inflammatory conditions for recruitment of naïve antigen presenting cells (APCs) such as dendritic cells (DCs) to sites of infection and/or vaccine administration. In this study, we examined the innate immune potential of primary LEC populations derived from multiple tissues of an animal model for human infectious diseases -- the ferret. We generated a total of six primary LEC populations from lung, tracheal, and mesenteric LN tissues from three different ferrets. Standard RT-PCR characterization of these primary LECs showed that they varied in their expression of LEC markers. The ferret LECs were examined for their ability to respond to poly I:C (TLR3 and RIG-1 ligand) and other known TLR ligands as measured by production of proinflammatory cytokine (IFNα, IL6, IL10, Mx1, and TNFα) and chemokine (CCL5, CCL20, and CXCL10) mRNAs using real time RT-PCR. Poly I:C exposure induced robust proinflammatory responses by all of the primary ferret LECs. Chemotaxis was performed to determine the functional activity of CCL20 produced by the primary lung LECs and showed that the LEC-derived CCL20 was abundant and functional. Taken together, our results continue to reveal the innate immune

Corresponding author, Todd A. Reinhart, ScD, 130 DeSoto St., Graduate School of Public Health, University of Pittsburgh, Pittsburgh, Pennsylvania, 15261, United States of America., Telephone: +1-412-648-2341, Fax: +1-412-624-4873.

potential of primary LECs during pathogen-host interactions and expand our understanding of the roles of LECs might play in health and disease in animal models.

indexing terms

Lymphatics; lymphatic endothelial cell; ferret; toll-like receptor; chemokine

Introduction

The lymphatic vasculature (LV) is often described as a network of unidirectional, blind-ended capillaries and larger collecting vessels made up of a single layer of loosely overlapping cells – lymphatic endothelial cells (LECs) (Jurisic and Detmar, 2009; Wang and Oliver, 2010). Since the LE is often located within micrometers beneath mucosal surfaces, they are likely to be among the first cells to participate in early host innate immune responses upon contact with microbes, host inflammatory signals, and vaccine antigens. LECs secrete chemoattractant cytokines (chemokines), such as CCL20, which recruit immature DCs to sites of inflammation, and CCL21, which draws antigen-loaded mature DCs into the collecting lymphatic vessels and then downstream into the LN paracortices, wherein a unique environment is created to optimize activation of adaptive immune responses (Luther et al., 2000; Saeki et al., 1999).

Model human LECs express functional toll-like receptors (TLRs) that recognize multiple pathogen-associated molecular patterns (PAMPs) on microbes (Garrafa et al., 2011; Pegu et al., 2008). TLR activation results in signaling that triggers the production of pro-inflammatory cytokines and chemokines, including type I interferons (IFNs), that are crucial not only for pathogen clearance during innate responses, but also enhance the induction of antigen-specific responses during subsequent adaptive immunity (Akira and Takeda, 2004; Beutler, 2009). Thus, the use of TLR ligands as vaccine adjuvants to increase vaccine efficacy in inducing host immune responses is an attractive strategy for development of next generation vaccines. Recent studies on the use of TLR ligand-conjugated vaccines have been promising in non-human primates(Kwissa et al., 2012) as well as small animal models such as mice (Zhang and Matlashewski, 2008; Zhu et al., 2010) and ferrets (Fang et al., 2010). However, different TLR ligand adjuvants mediate distinct cellular and molecular profiles of early innate responses in the periphery and the lymphatic organs of non-human primates (Kwissa et al., 2012). Despite their potential, there is still limited understanding of the local and systemic immune responses and potential toxicities associated with their use in vivo.

Ferrets are becoming an increasingly examined small animal model for the study of human diseases, including neurobiology (Atkinson et al., 1989; Bock et al., 2010; Medina et al., 2005), cancer (Kim et al., 2006), and infectious diseases of viral and bacterial origin (Chu et al., 2008; Geisbert et al., 2010; Martina et al., 2003; Svitek and von Messling, 2007; Woods et al., 2002). The use of the ferret as an animal model for studying human respiratory diseases has offered a number of advantages. First, ferret airways resemble and share many anatomical and physiological similarities to humans making them useful for study of human respiratory infections (Bruder et al., 2010). In addition, ferrets are highly susceptible to a

number of human respiratory pathogens that often require no laboratory adaptation prior to infection (Belser et al., 2011; O'Donnell and Subbarao, 2011). Furthermore, ferrets are considered an accurate small animal model to study both human and avian influenza (Bouvier and Lowen, 2010). In this regard, the ferret model is used to study not only seasonal and highly pathogenic avian influenza virus pathogenicity, but also viral transmission (Herfst et al., 2012; Russell et al., 2012) and the development of vaccines and antiviral therapeutics (Banner and Kelvin, 2012).

Despite the utility and increasing use of this animal model there is still a major lack of ferret-specific reagents for use in research, despite efforts that have been invested to obtain reagents to enable development of ferret-specific assays at the cellular and molecular levels (Bruder et al., 2010; Camp et al., 2012). Molecular cloning and phylogenetic analysis of ferret immune-related genes provides tools to assess the inflammatory cytokine and chemokine profiles in infected animals and determine their importance in disease progression and/or clearance of infection (Nakata et al., 2008; Qin et al., 2013). The expression of functional TLRs by human LECs (Pegu et al., 2008) has highlighted that the LE could be a target for new vaccine adjuvancy strategies, alongside monocytes and DCs. In this light, we isolated, cultured, and characterized primary LECs from multiple ferret tissues, and determined their responsiveness to known TLR ligands by measuring the production of proinflammatory cytokine and chemokine mRNAs using real time RT-PCR. In addition, we also cloned and sequenced ferret LEC marker partial cDNAs for in situ hybridization (ISH) analysis to probe the lymphatic vasculature in ferret tissues. Altogether, these findings provide insight into the function and microanatomy of ferret lymphatics and establish a foundation for examination of the roles of LECs during infection and immunization.

Methods

Ferrets and Tissue Processing

The ferrets from which tissues for histological analysis and isolation of LECs were obtained were available from other non-infectious studies, and were 6–7 month old females that ranged in weight from 695–825g. These ferrets were vaccinated for Canine Distemper virus, descented, and single housed at the University of Pittsburgh. All animal work was approved by the University of Pittsburgh Institutional Animal Care and Use Committee, although the tissues contributing to these studies were excess tissues available at necropsy.

RT-PCR, cloning, and phylogenetic analysis of ferret LEC markers

Due to the lack of complete ferret genomic sequence information, design of ferret-specific primers for amplification of ferret cDNAs, including LEC markers (Table 1), was based on published canine sequences available in GenBank, National Center for Biotechnology Information (NCBI). Previous analyses of ferret cytokine cDNAs reported that ferret sequences were closely related to canine sequences (Nakata et al., 2008). Total cellular RNAs were obtained from ferret lung, spleen, and LN tissues, both untreated and stimulated overnight with unmethylated CpG oligonucleotides (ODN), poly I:C, or lipopolysaccharide (LPS). RNA extractions were performed using Trizol (Life Technologies, Rockville, MA, USA) according to the manufacturer’s recommendation. Total RNA (2 μg) was reverse

transcribed using oligo-dT primer (Promega, Madison, MI, USA) and avian myeloblastosis virus reverse transcriptase (Promega, Madison, MI, USA). The resulting cDNAs for each tissue type were pooled and standard RT-PCR was performed using GoTaq DNA Polymerase (Promega, Madison, MI, USA) with ferret-specific primers (Table 2) using PCR conditions as follows: 94°C for 3 min, 94°C for 30 sec, 58°C for 30 sec, and 72°C 2 min for 35 cycles, followed by 72°C for an additional 10 min before holding at 4°C. Amplified products were run on a 1% agarose gel prestained with GelRed™ Nucleic Acid Stain (Invitrogen, Carlsbad, CA, USA). PCR products were purified from gel slices using the QIAEX II gel extraction kit (QIAGEN, USA) before subcloning into the pGEMT cloning vector (Promega, Madison, MI, USA). The inserts were sequence verified and analyzed using the Vector NTI program (Invitrogen, Life Technologies). Sequences were aligned with corresponding sequences from other species as available through the NCBI/GenBank database using the ClustalX 2.1 multiple sequence alignment program (Jeanmougin et al., 1998). Phylogenetic trees were generated by the neighbor-joining method after DNA distance calculation using the PHYLIP 3.69 program (Felsenstein, 1989), and drawn with Tree View 1.6.6 (Page, 1996).

Isolation and culture of primary ferret lymphatic endothelial cells from tissues

LEC isolation was performed as described (Nisato et al., 2009). Briefly, ferret tissues were mechanically digested by mincing with sterile surgical scissors, followed by enzymatic digestion with 0.25% trypsin overnight at 4°C. Digested cells were passed through a 100 μM cell strainer once, and twice through 70 μM cell strainers. Primary LECs were cultured on rat tail collagen I (BD Biosciences) coated culture dishes using the EGM2 endothelial specialized medium (Lonza), supplemented with 2% FBS, and a final concentration of 100 ng/ml recombinant human VEGF-C (R&D Systems, Minneapolis, MN, USA). Cells were grown at 37°C with 5% CO_2 until they reached 80–90% confluency, and then passaged at between 1:4 to 1:8 splits. The resulting cell populations were characterized by standard RT-PCR using primers specific for ferret LEC markers (Table 2) using PCR conditions described above.

Stimulation of ferret LECs with TLR ligands

Near confluent monolayers (80–90%) of primary ferret LECs were exposed to ligands for TLRs 1 to 9 (InvivoGen, San Diego, CA, USA) in parallel with mock treated cultures for each LEC population. Concentrations of TLR agonists were as described (Pegu et al., 2008). After 24 hr of treatment, total RNA extractions were performed using Trizol (Life Technologies, Rockville, MA, USA) according to the manufacturer's recommendation. Statistical analyses were performed using the Prism software package (GraphPad, San Diego, CA). Paired *t*-tests were used to compare mock versus TLR ligand treated samples because no nonparametric method for paired data can be properly applied to sample size less than 6. A *p*-value of <0.05 was considered significant.

Real-time RT-PCR

Primers for real-time RT-PCR measurement of podoplanin, LYVE-1, and CCL20 mRNA levels were design based on the ferret sequences presented here (Table 2). Primers for

GAPDH, CCL5, CXCL10, IFN-α, IL6, IL10, TNFα, and Mx1 were obtained from published studies.(Fang et al., 2010; Nakata et al., 2009) SYBR Green real-time RT-PCR (comparative Ct method) was performed on an ABI Prism 7000 Sequence Detection System (Applied Biosystems) as described (Sanghavi and Reinhart, 2005). All samples were assayed in duplicate and with concurrent controls that lacked reverse transcriptase in the cDNA synthesis reaction.

Chemotaxis

Chemotaxis assay was performed using murine L1.2 cells engineered to express ferret CCR6 as described (Qin et al., 2013). Briefly, a total of 200,000 of L1.2.fCCR6 responder cells were loaded on top of the porous membrane (ChemoTx® Disposable Chemotaxis System, pore size 5 μm, NeuroProbe) in triplicate and incubated at 37°C/5% CO_2 for 2 hr in a humid chamber. The number of migrating cells was counted using a hemacytometer. Chemotactic index (CI) was calculated relative to control wells with no chemokine. Chemically synthesized ferret CCL20 (Qin et al., 2013) was used as a control.

In situ hybridization (ISH)

Paraffin embedded ferret tissue sections were cut at 5 μM and mounted on Superfrost Plus slides (Bio-Optica). ^{35}S-UTP-labeled riboprobes were generated (Pegu et al., 2007) and used for stringent ISH on ferret tissues. Autoradiographic exposure times for ferret specific LEC markers after ISH were 14 days for LYVE-1 and CCL21 mRNA targets and 21 days for podoplanin, PROX-1, and VEGFR-3 mRNA targets. We note that for reasons not yet clear, in these studies and others, ISHs with many probes in ferret tissues have resulted in marginally acceptable signal-to-noise ratios.

Results

Cloning, sequencing, and phylogenetic analysis of ferret LEC marker cDNAs

Given the paucity of ferret-specific or cross-reactive reagents available for research, particularly for lymphatic analyses, we designed primers for use in RT-PCRs to acquire ferret LEC marker partial cDNAs based on published canine sequences, a species highly related to the ferret (Nakata et al., 2008; Qin et al., 2013). These studies were driven by the goal of obtaining primary ferret LECs for ex vivo analyses (below) and it was imperative to obtain information on LEC target sequences to allow development of assays for measurement of mRNA levels in the LEC populations. We successfully obtained cDNAs containing full-length (podoplanin and CCL21) or partial (LYVE-1, PROX-1, and VEGFR-3) ORFs from total cellular RNAs prepared from ferret tissues. Sequence homology analysis of each of the ferret LEC markers with other species showed the highest similarity to the order *Carnivora*, with *Canis lupus* being the most related species (Table 1). This corroborated earlier findings with ferret immune-related genes (Nakata et al., 2008; Qin et al., 2013). Ferret LEC markers shared between 74% to 98% sequence homology to the corresponding human sequences at the nucleotide level and between 60% to 100% sequence homology at the amino acid level. Analysis of the PROX-1 partial ORF showed it is well conserved across multiple species at both the nucleotide (98%) and amino acid (99–100%) levels. Phylogenetic analysis of the podoplanin complete ORF revealed that ferret sequences

clustered together with species in the order *Carnivora* (Figure 1). Phylogenetic trees constructed for the other ferret LEC markers revealed highly similar results (data not shown).

Isolation and characterization of primary ferret LECs

To obtain LECs from ferrets, we isolated a total of six primary ferret LEC populations from three different ferrets and four different tissue types (skin, lung, trachea, and mesenteric LN). Cultured primary ferret LECs formed confluent monolayers approximately 10 to 14 days after initial plating onto collagen-coated plastic surfaces, these cultures being designated as passage zero (P0). The primary ferret LEC monolayers showed the typical cobbled-stone morphology of endothelial cells observed in conventional 2D culture systems (data not shown).

The primary cultures were characterized first by standard RT-PCR for expression of the LEC markers podoplanin, LYVE-1, PROX-1, VEGFR-3, and CCL21 (Figure 2). All of the primary ferret LEC populations isolated from all tissues types expressed podoplanin and PROX-1 mRNAs to high levels. In contrast, the expression of LYVE-1 and VEGFR-3 varied among the LEC populations. LYVE-1 expression was not detected in the primary ferret LECs isolated from skin (F1 skin), whereas VEGFR-3 expression was not detected in the skin (F1 skin) and trachea (F2 trachea) LEC populations. CCL21 mRNA was detected in all cultured primary ferret LECs, although the CCL21-specific primers yielded two differently sized bands. Gel extraction and sequencing of both bands revealed that the larger fragment contained all sequences present in the smaller fragment as well as what was likely an additional intron, consistent with alternative splicing of an mRNA precursor.

Ferret LECs respond to TLR ligand stimulation

To determine whether the ferret LECs responded to PAMPs, we first exposed all LEC populations for 24 hr to poly I:C, a double-stranded viral mimetic and a known TLR3 and RIG-I ligand,. Since two of the primary lung LEC populations were derived from the same ferret and revealed similar LEC marker expression profiles by standard RT-PCR, we included just one of the populations in these and subsequent studies. Responsiveness was assessed by measurement of proinflammatory cytokine (TNFα, IFNα, IL6, and IL10), chemokine (CCL5, CCL20, and CXCL10), and IFN-stimulated gene (ISG) Mx1 mRNA levels using newly designed or published (Fang et al., 2010; Nakata et al., 2008) ferret-specific real-time RT-PCR primers (Table 2). All primary ferret LEC populations responded to poly I:C, with increases in levels of all eight mRNAs examined ($p<0.05$ for all mRNAs; Figure 3). The levels in increase ranged from 5-fold (IL-10) to 633,031-fold (Mx1), as determined from the ratio of the geometric means for the treated and control groups.

To determine further whether LECs derived from lung tissues, which comprise a major host/pathogen/environment interface, are responsive to multiple TLR ligands, one of the primary ferret lung LEC populations (F2 lung LEC, left lobe) was exposed to different TLR ligands (TLR1-9) for 24 hr. Responsiveness was measured again by real time RT-PCR. The ferret lung LECs responded strongly to most of the TLR ligands examined (Figure 4), although this varied depending upon the TLR ligand and the mRNA measured. The gene showing the

greatest overall response across TLR ligands was CCL20 (Figure 4) with a mean induction (geometric mean) of 5,041-fold across all TLR ligands. In contrast, the mean induction levels for TNF-α, IFN-α, and IL-10 were all less than 1.5-fold across all TLR ligands. Analysis of the LEC responses across all genes for the individual TLR ligands revealed that poly I:C was the most potent TLR ligand under these conditions inducing the eight genes examined an average of 2,424-fold (geometric mean). The low molecular weight form of poly I:C induced these genes an average of 288-fold. In contrast, all of the other TLR ligands induced the same genes only 0.9-fold (LPS and flagellin) to 10.2-fold (FSL-1).

To unveil possible relations among the mRNA expression changes induced in the ferret LECs by TLR ligands, we performed Spearman correlation analyses (Table 3). Pairwise correlation analyses revealed that IL-6 mRNA levels correlated with four other mRNAs (CCL5, CCL20, CXCL10, and Mx1). Similarly CXCL10, CCL5, and CCL20 mRNA levels were all positively correlated with each other and with a total of three other mRNAs. Amongst this small set of host response genes, the levels of IFN-α, TNF-α, and IL-10 were not correlated with the levels of any other mRNAs (Table 3). The lack of correlation between IFN-α and the ISGs CXCL10 and Mx1 was surprising, but induction of other IFNs like drove the induction of these two ISGs. Additionally, these collective analyses are complicated by the analysis of this data set driven by stimulation and signaling through nine different TLRs and their respective signaling pathways.

Primary ferret lung LECs stimulated with TLR ligands produce functional CCL20

Given that the chemokine CCL20 was the most responsive of the genes examined after TLR stimulation, and that we have previously developed a chemotaxis assay for ferret CCL20 (Qin et al., 2013), we measured the CCR6-responsive activities of supernatants collected from the TLR ligand treated LECs. Chemically synthesized ferret CCL20 protein was used as a positive control for cell migration and media alone was used as a negative control. Migration of the ferret CCR6+ responder cells to serial dilutions of the synthetic peptide generated the typical bell-shaped, dose-dependent responses (Figure 5, right), with maximum migration at 10nM, yielding a chemotactic index (CI) of 393 (with 20,000–30,000 cells typically migrating). Among the TLR ligands examined, the supernatant from the Pam3CSK-treated LECs induced the greatest cell migration with a CI of 169, followed by supernatant from the FSL-1-treated cells (CI of 162), poly I:C-treated cells (CI of 111), flagellin-treated cells (CI of 27), and ssRNA40-treated cells (CI of 30). Although the real-time RT-PCR data showed that all of the TLR ligands increased the levels of CCL20 mRNA (Figure 4), although only five out of eight LEC-stimulated culture supernatants recruited ferret CCR6+ responder cells above medium alone. It is possible that the concentrations of CCL20 protein in the other LEC culture supernatants were at or higher than 1 μM, which is a concentration above which a responder cell is unable to distinguish a concentration gradient from the front and the back of the cell (Figure 5, right).

Distribution of LEC markers in ferret tissues

Given the essential role of the LE for transport of soluble antigens and immune cells for host responses and immune surveillance, we examined the distribution of the LV in multiple ferret tissues by using in situ hybridization (ISH). To do this, we generated ^{35}S-radiolabeled

riboprobe for detection of ferret LE-associated mRNAs in ferret LN, lung, spleen, and jejunal tissues.

These attempts to map the LV in ferret tissues using podoplanin or VEGFR-3 specific ISH probes was complicated by high background signals and low specific signals, whereas the LYVE-1 and CCL21 probes yielded signals that were reasonable and robust, respectively. In LN tissues, these ISHs revealed a distribution of LYVE-1 mRNA at the subcapsular sinus (Figure 6) with limited expression in LN parenchyma, consistent with expression by the LV. In LN, CCL21 mRNA was abundant in the cortical and paracortical regions (not shown) as we (Pegu et al., 2007) and others have observed in other animals models. In jejunum, LYVE-1 (Figure 6) and CCL21 (not shown) were in the lacteals of villi, which are part of the LV immediately beneath the intestinal epithelium. We also observed networks of LV expressing high levels of CCL21 in the jejunal smooth muscle layer (not shown). In lung tissues, ferret CCL21 mRNA was expressed by widely distributed, small, thin-walled vessels in areas near (Figure 6) and distal to conducting airways. Parallel hybridization of subjacent tissue sections with a sense control riboprobe yielded no specific signal for any of the tissues examined (Figure 6). Overall these findings provide a first analysis of lymphatic structure in ferret tissues and reveal the LV to be widely distributed in ferret lung.

Discussion

The LV system is a critically important vascular system that drains interstitial fluids, particulates, and cells from peripheral tissues, disruption of which leads to lymphedema. Despite serving this important function, the LECs that serve as the major constituents of lymphatic vessels are understudied in comparison to their counterparts, blood endothelial cells (BECs), in blood vessels. Identification of LEC markers has facilitated research on LECs and helped in distinguishing them from BEC. The findings presented here describe the first isolation, culture, and functional characterization of ferret LECs, paving the way for studying LEC contributions to health and disease processes in ferret models.

An approach used for isolation and characterization of primary LECs from humans, mice, or rats involves mechanical and enzymatic dissociation of tissues followed by enrichment using LEC marker-specific antibodies (Ando et al., 2005; Garrafa et al., 2006; Kriehuber et al., 2001; Sironi et al., 2006). Due to lack of ferret-specific or cross-reactive LEC marker-specific antibodies we were unable to enrich primary ferret LECs. Not surprisingly, though, immunosorting of LECs using marker-specific antibodies can contribute to differences observed in the molecular and functional profiles of isolated LECs (Whitehurst et al., 2006), which could be expected to be heterogeneous in different anatomic and microanatomic compartments. Therefore, it will be important to keep in mind this potential for bias towards enrichment of subpopulations of LECs expressing moderate to high levels of surface antigens (Whitehurst et al., 2006). On the other hand, cell types other than LECs can express the markers used for enrichment (Wick et al., 2008), such as with LYVE-1, which is expressed by heterogeneous populations of cells, including subpopulations expressing CD68, CD206, or CD208 (Ogunbiyi et al., 2011), which in turn could lead to inclusion of non-LECs in the immune-enriched populations obtained and studied. A recent study showed that LECs obtained by digesting pooled brachial, axillary, inguinal, and popliteal LNs from

wild-type C57BL/6J mouse and simple bulk culture in the common DMEM medium, yielded LECs that preserved their LEC characteristics over at least 20 passages (Jordan-Williams and Ruddell, 2014).

The LE is actively involved in the regulation of cellular traffic from peripheral tissues to draining LNs, which is important for the initiation and maintenance of antigen-specific immune responses during infection and vaccination. Primary human LECs express functional TLRs that sense PAMPs and secrete proinflammatory cytokines and chemokines at peripheral sites for recruitment of APCs to and through the LV (Johnson and Jackson, 2010; Pegu et al., 2008). However, little is known about primary LECs from other species commonly used as animal models for human diseases. The ferret is an attractive small animal model to study human respiratory viruses, especially influenza virus, due to the unique physiologic and anatomic similarities of its respiratory tract relative to humans (Belser et al., 2011; Bouvier and Lowen, 2010; Geisbert et al., 2010; O'Donnell and Subbarao, 2011). The ferret model has been utilized as an animal model to study seasonal and avian influenza virus pathogenesis, as well for vaccine and therapeutic development and studies of viral transmission (Banner and Kelvin, 2012; Herfst et al., 2012; Leon et al., 2013; Russell et al., 2012). We describe here for the first time the isolation of primary ferret LECs and their responses to TLR ligands. A comprehensive analysis of ferret lung LEC responses to TLR1-9 ligands revealed that they respond to a large repertoire of TLR ligands. This ability to recognize and respond to a diverse set of microbes is consistent with our previous findings with commercially obtained human LECs (Pegu et al., 2008). This information will be useful in extrapolating information on LEC-involved host responses to infection and mechanisms of vaccine-mediated protection in ferret animal models to humans.

Due to its primary function in gas exchange the lung is widely exposed to the external environment and to diverse microorganisms. The lung, however, has evolved a number of mechanical and physiological barriers that inhibit colonization by pathogenic microbes (Yoo et al., 2013). There is a necessarily delicate balance in the lung among the different host immune responses, including inflammation (La Gruta et al., 2007). Initiation of host immune responses against invading pathogens in the lung mucosal surface requires recognition of PAMPs and activation of complement and other innate and then adaptive immune responses. At the same time, exacerbation of these responses through overproduction of proinflammatory cytokines and chemokines could result in severe immunopathological damage to the lung. Recent studies have provided evidence for the direct involvement of the lymphatics in both the induction and the resolution of inflammation (Chaitanya et al., 2010; McKimmie et al., 2013; Wilting et al., 2009). Such findings can provide assistance in the development of strategies to modulate innate immune responses to limit inflammation and lung injury during infection. Chemokines are important mediators of host homeostatic processes and also of host immune responses to pathogens. However, chemokines, such as CCL20, can contribute to the pathology of a number of chronic and severe inflammatory pulmonary diseases (Demedts et al., 2007; Lukacs et al., 2001). We have shown here that TLR stimulation of ferret lung LECs led to high levels of production of functional CCL20. The CCL20 and overall patterns of responsiveness to TLR ligands were similar to that of human pulmonary LECs (Pegu et al., 2008). Given that the receptor for CCL20, CCR6, is expressed on immature DCs and IL-17-producing Th17 cells

(Singh et al., 2008), LECs could play fundamental direct and indirect roles in immune surveillance and mucosal homeostasis.

In summary, our findings represent the first isolation and functional characterization of LECs isolated from ferret, an increasingly commonly used animal model for human diseases. In addition, these cells and supporting cDNA resources provide a foundation for deeper studies of lymphatic structure and function in ferrets. Our data also report for the first time a comprehensive analysis of the TLR ligand responsiveness of ferret lung LECs. These observations provide further evidence that the LV is not simply a passive conduit, but that LECs have more active roles in induction of host innate immune responses and in regulation of inflammation after infection. In sum, the LV presents ongoing opportunities for development of improved vaccine, infection control, and inflammation control strategies.

Supplementary Material

Refer to Web version on PubMed Central for supplementary material.

Acknowledgements

We thank Dr. Ted Ross for provision of ferret tissues. This study was funded by NIH Grant (AI074509 to DHF). Stella J. Berendam was supported in large part by the Ministry of Science, Technology, and Innovation (MOSTI), Government of Malaysia and the Department of Infectious Diseases and Microbiology and Center for Lymphatic Immunobiology, Graduate School of Public Health, University of Pittsburgh.

References

Akira S, Takeda K. Toll-like receptor signalling. Nature reviews. Immunology. 2004; 4:499–511. [PubMed: 15229469]

Ando T, Jordan P, Joh T, Wang Y, Jennings MH, Houghton J, Alexander JS. Isolation and characterization of a novel mouse lymphatic endothelial cell line: SV-LEC. Lymphat Res Biol. 2005; 3:105–115. [PubMed: 16190815]

Atkinson CS, Press GA, Lyden P, Katz B. The ferret as an animal model in cerebrovascular research. Stroke; a journal of cerebral circulation. 1989; 20:1085–1088.

Banner D, Kelvin AA. The current state of H5N1 vaccines and the use of the ferret model for influenza therapeutic and prophylactic development. Journal of infection in developing countries. 2012; 6:465–469. [PubMed: 22706187]

Belser JA, Katz JM, Tumpey TM. The ferret as a model organism to study influenza A virus infection. Disease models & mechanisms. 2011; 4:575–579. [PubMed: 21810904]

Beutler B. Microbe sensing, positive feedback loops, and the pathogenesis of inflammatory diseases. Immunological reviews. 2009; 227:248–263. [PubMed: 19120489]

Bock AS, Olavarria JF, Leigland LA, Taber EN, Jespersen SN, Kroenke CD. Diffusion tensor imaging detects early cerebral cortex abnormalities in neuronal architecture induced by bilateral neonatal enucleation: an experimental model in the ferret. Frontiers in systems neuroscience. 2010; 4:149. [PubMed: 21048904]

Bouvier NM, Lowen AC. Animal Models for Influenza Virus Pathogenesis and Transmission. Viruses. 2010; 2:1530–1563. [PubMed: 21442033]

Bruder CE, Yao S, Larson F, Camp JV, Tapp R, McBrayer A, Powers N, Granda WV, Jonsson CB. Transcriptome sequencing and development of an expression microarray platform for the domestic ferret. BMC genomics. 2010; 11:251. [PubMed: 20403183]

Camp JV, Svensson TL, McBrayer A, Jonsson CB, Liljestrom P, Bruder CE. De-novo transcriptome sequencing of a normalized cDNA pool from influenza infected ferrets. PloS one. 2012; 7:e37104. [PubMed: 22606336]

Chaitanya GV, Franks SE, Cromer W, Wells SR, Bienkowska M, Jennings MH, Ruddell A, Ando T, Wang Y, Gu Y, Sapp M, Mathis JM, Jordan PA, Minagar A, Alexander JS. Differential cytokine responses in human and mouse lymphatic endothelial cells to cytokines in vitro. Lymphat Res Biol. 2010; 8:155–164. [PubMed: 20863268]

Chu YK, Ali GD, Jia F, Li Q, Kelvin D, Couch RC, Harrod KS, Hutt JA, Cameron C, Weiss SR, Jonsson CB. The SARS-CoV ferret model in an infection-challenge study. Virology. 2008; 374:151–163. [PubMed: 18234270]

Demedts IK, Bracke KR, Van Pottelberge G, Testelmans D, Verleden GM, Vermassen FE, Joos GF, Brusselle GG. Accumulation of dendritic cells and increased CCL20 levels in the airways of patients with chronic obstructive pulmonary disease. American journal of respiratory and critical care medicine. 2007; 175:998–1005. [PubMed: 17332482]

Fang Y, Rowe T, Leon AJ, Banner D, Danesh A, Xu L, Ran L, Bosinger SE, Guan Y, Chen H, Cameron CC, Cameron MJ, Kelvin DJ. Molecular characterization of in vivo adjuvant activity in ferrets vaccinated against influenza virus. Journal of virology. 2010; 84:8369–8388. [PubMed: 20534862]

Felsenstein J. Mathematics vs. Evolution: Mathematical Evolutionary Theory. Science. 1989; 246:941–942. [PubMed: 17812579]

Garrafa E, Alessandri G, Benetti A, Turetta D, Corradi A, Cantoni AM, Cervi E, Bonardelli S, Parati E, Giulini SM, Ensoli B, Caruso A. Isolation and characterization of lymphatic microvascular endothelial cells from human tonsils. J Cell Physiol. 2006; 207:107–113. [PubMed: 16261591]

Garrafa E, Imberti L, Tiberio G, Prandini A, Giulini SM, Caimi L. Heterogeneous expression of toll-like receptors in lymphatic endothelial cells derived from different tissues. Immunology and cell biology. 2011; 89:475–481. [PubMed: 20921966]

Geisbert TW, Daddario-DiCaprio KM, Hickey AC, Smith MA, Chan YP, Wang LF, Mattapallil JJ, Geisbert JB, Bossart KN, Broder CC. Development of an acute and highly pathogenic nonhuman primate model of Nipah virus infection. PloS one. 2010; 5:e10690. [PubMed: 20502528]

Herfst S, Schrauwen EJ, Linster M, Chutinimitkul S, de Wit E, Munster VJ, Sorrell EM, Bestebroer TM, Burke DF, Smith DJ, Rimmelzwaan GF, Osterhaus AD, Fouchier RA. Airborne transmission of influenza A/H5N1 virus between ferrets. Science. 2012; 336:1534–1541. [PubMed: 22723413]

Jeanmougin F, Thompson JD, Gouy M, Higgins DG, Gibson TJ. Multiple sequence alignment with Clustal X. Trends in biochemical sciences. 1998; 23:403–405. [PubMed: 9810230]

Johnson LA, Jackson DG. Inflammation-induced secretion of CCL21 in lymphatic endothelium is a key regulator of integrin-mediated dendritic cell transmigration. Int Immunol. 2010; 22:839–849. [PubMed: 20739459]

Jordan-Williams KL, Ruddell A. Culturing Purifies Murine Lymph Node Lymphatic Endothelium. Lymphat Res Biol. 2014

Jurisic G, Detmar M. Lymphatic endothelium in health and disease. Cell and tissue research. 2009; 335:97–108. [PubMed: 18648856]

Kim Y, Liu XS, Liu C, Smith DE, Russell RM, Wang XD. Induction of pulmonary neoplasia in the smoke-exposed ferret by 4-(methylnitrosamino)-1-(3-pyridyl)-1-butanone (NNK): a model for human lung cancer. Cancer letters. 2006; 234:209–219. [PubMed: 15894421]

Kriehuber E, Breiteneder-Geleff S, Groeger M, Soleiman A, Schoppmann SF, Stingl G, Kerjaschki D, Maurer D. Isolation and characterization of dermal lymphatic and blood endothelial cells reveal stable and functionally specialized cell lineages. J Exp Med. 2001; 194:797–808. [PubMed: 11560995]

Kwissa M, Nakaya HI, Oluoch H, Pulendran B. Distinct TLR adjuvants differentially stimulate systemic and local innate immune responses in nonhuman primates. Blood. 2012; 119:2044–2055. [PubMed: 22246032]

La Gruta NL, Kedzierska K, Stambas J, Doherty PC. A question of self-preservation: immunopathology in influenza virus infection. Immunology and cell biology. 2007; 85:85–92. [PubMed: 17213831]

Leon AJ, Banner D, Xu L, Ran L, Peng Z, Yi K, Chen C, Xu F, Huang J, Zhao Z, Lin Z, Huang SH, Fang Y, Kelvin AA, Ross TM, Farooqui A, Kelvin DJ. Sequencing, annotation, and

characterization of the influenza ferret infectome. Journal of virology. 2013; 87:1957–1966. [PubMed: 23236062]

Lukacs NW, Prosser DM, Wiekowski M, Lira SA, Cook DN. Requirement for the chemokine receptor CCR6 in allergic pulmonary inflammation. The Journal of experimental medicine. 2001; 194:551–555. [PubMed: 11514610]

Luther SA, Tang HL, Hyman PL, Farr AG, Cyster JG. Coexpression of the chemokines ELC and SLC by T zone stromal cells and deletion of the ELC gene in the plt/plt mouse. Proceedings of the National Academy of Sciences of the United States of America. 2000; 97:12694–12699. [PubMed: 11070085]

Martina BE, Haagmans BL, Kuiken T, Fouchier RA, Rimmelzwaan GF, Van Amerongen G, Peiris JS, Lim W, Osterhaus AD. Virology: SARS virus infection of cats and ferrets. Nature. 2003; 425:915. [PubMed: 14586458]

McKimmie CS, Singh MD, Hewit K, Lopez-Franco O, Le Brocq M, Rose-John S, Lee KM, Baker AH, Wheat R, Blackbourn DJ, Nibbs RJ, Graham GJ. An analysis of the function and expression of D6 on lymphatic endothelial cells. Blood. 2013; 121:3768–3777. [PubMed: 23479571]

Medina AE, Krahe TE, Ramoa AS. Early alcohol exposure induces persistent alteration of cortical columnar organization and reduced orientation selectivity in the visual cortex. Journal of neurophysiology. 2005; 93:1317–1325. [PubMed: 15483067]

Nakata M, Itou T, Sakai T. Molecular cloning and phylogenetic analysis of inflammatory cytokines of the ferret (Mustela putorius furo). The Journal of veterinary medical science / the Japanese Society of Veterinary Science. 2008; 70:543–550. [PubMed: 18628593]

Nakata M, Itou T, Sakai T. Quantitative analysis of inflammatory cytokines expression in peripheral blood mononuclear cells of the ferret (Mustela putorius furo) using real-time PCR. Veterinary immunology and immunopathology. 2009; 130:88–91. [PubMed: 19157571]

Nisato RE, Buser R, Pepper MS. Lymphatic endothelial cells: establishment of primaries and characterization of established lines. Methods Mol Biol. 2009; 467:113–126. [PubMed: 19301667]

O'Donnell CD, Subbarao K. The contribution of animal models to the understanding of the host range and virulence of influenza A viruses. Microbes and infection / Institut Pasteur. 2011; 13:502–515. [PubMed: 21276869]

Ogunbiyi S, Chinien G, Field D, Humphries J, Burand K, Sawyer B, Jeffrey S, Mortimer P, Clasper S, Jackson D, Smith A. Molecular characterization of dermal lymphatic endothelial cells from primary lymphedema skin. Lymphat Res Biol. 2011; 9:19–30. [PubMed: 21417764]

Page RD. TreeView: an application to display phylogenetic trees on personal computers. Comput Appl Biosci. 1996; 12:357–358. [PubMed: 8902363]

Pegu A, Flynn JL, Reinhart TA. Afferent and efferent interfaces of lymph nodes are distinguished by expression of lymphatic endothelial markers and chemokines. Lymphat Res Biol. 2007; 5:91–103. [PubMed: 17935477]

Pegu A, Qin S, Fallert Junecko BA, Nisato RE, Pepper MS, Reinhart TA. Human lymphatic endothelial cells express multiple functional TLRs. J Immunol. 2008; 180:3399–3405. [PubMed: 18292566]

Qin S, Klamar CR, Fallert Junecko BA, Craigo J, Fuller DH, Reinhart TA. Functional characterization of ferret CCL20 and CCR6 and identification of chemotactic inhibitors. Cytokine. 2013; 61:924–932. [PubMed: 23360828]

Russell CA, Fonville JM, Brown AE, Burke DF, Smith DL, James SL, Herfst S, van Boheemen S, Linster M, Schrauwen EJ, Katzelnick L, Mosterin A, Kuiken T, Maher E, Neumann G, Osterhaus AD, Kawaoka Y, Fouchier RA, Smith DJ. The potential for respiratory droplet-transmissible A/H5N1 influenza virus to evolve in a mammalian host. Science. 2012; 336:1541–1547. [PubMed: 22723414]

Saeki H, Moore AM, Brown MJ, Hwang ST. Cutting edge: secondary lymphoid-tissue chemokine (SLC) and CC chemokine receptor 7 (CCR7) participate in the emigration pathway of mature dendritic cells from the skin to regional lymph nodes. J Immunol. 1999; 162:2472–2475. [PubMed: 10072485]

Sanghavi SK, Reinhart TA. Increased expression of TLR3 in lymph nodes during simian immunodeficiency virus infection: implications for inflammation and immunodeficiency. J Immunol. 2005; 175:5314–5323. [PubMed: 16210637]

Singh SP, Zhang HH, Foley JF, Hedrick MN, Farber JM. Human T cells that are able to produce IL-17 express the chemokine receptor CCR6. J Immunol. 2008; 180:214–221. [PubMed: 18097022]

Sironi M, Conti A, Bernasconi S, Fra AM, Pasqualini F, Nebuloni M, Lauri E, De Bortoli M, Mantovani A, Dejana E, Vecchi A. Generation and characterization of a mouse lymphatic endothelial cell line. Cell Tissue Res. 2006; 325:91–100. [PubMed: 16534603]

Svitek N, von Messling V. Early cytokine mRNA expression profiles predict Morbillivirus disease outcome in ferrets. Virology. 2007; 362:404–410. [PubMed: 17289104]

Wang Y, Oliver G. Current views on the function of the lymphatic vasculature in health and disease. Genes & development. 2010; 24:2115–2126. [PubMed: 20889712]

Whitehurst B, Eversgerd C, Flister M, Bivens CM, Pickett B, Zawieja DC, Ran S. Molecular profile and proliferative responses of rat lymphatic endothelial cells in culture. Lymphat Res Biol. 2006; 4:119–142. [PubMed: 17034293]

Wick N, Haluza D, Gurnhofer E, Raab I, Kasimir MT, Prinz M, Steiner CW, Reinisch C, Howorka A, Giovanoli P, Buchsbaum S, Krieger S, Tschachler E, Petzelbauer P, Kerjaschki D. Lymphatic precollectors contain a novel, specialized subpopulation of podoplanin low, CCL27-expressing lymphatic endothelial cells. Am J Pathol. 2008; 173:1202–1209. [PubMed: 18772332]

Wilting J, Becker J, Buttler K, Weich HA. Lymphatics and inflammation. Current medicinal chemistry. 2009; 16:4581–4592. [PubMed: 19903150]

Woods JB, Schmitt CK, Darnell SC, Meysick KC, O'Brien AD. Ferrets as a model system for renal disease secondary to intestinal infection with Escherichia coli O157:H7 and other Shiga toxin-producing E. coli. The Journal of infectious diseases. 2002; 185:550–554. [PubMed: 11865409]

Yoo JK, Kim TS, Hufford MM, Braciale TJ. Viral infection of the lung: Host response and sequelae. J Allergy Clin Immunol. 2013

Zhang WW, Matlashewski G. Immunization with a Toll-like receptor 7 and/or 8 agonist vaccine adjuvant increases protective immunity against Leishmania major in BALB/c mice. Infection and immunity. 2008; 76:3777–3783. [PubMed: 18474642]

Zhu Q, Egelston C, Gagnon S, Sui Y, Belyakov IM, Klinman DM, Berzofsky JA. Using 3 TLR ligands as a combination adjuvant induces qualitative changes in T cell responses needed for antiviral protection in mice. The Journal of clinical investigation. 2010; 120:607–616. [PubMed: 20101095]

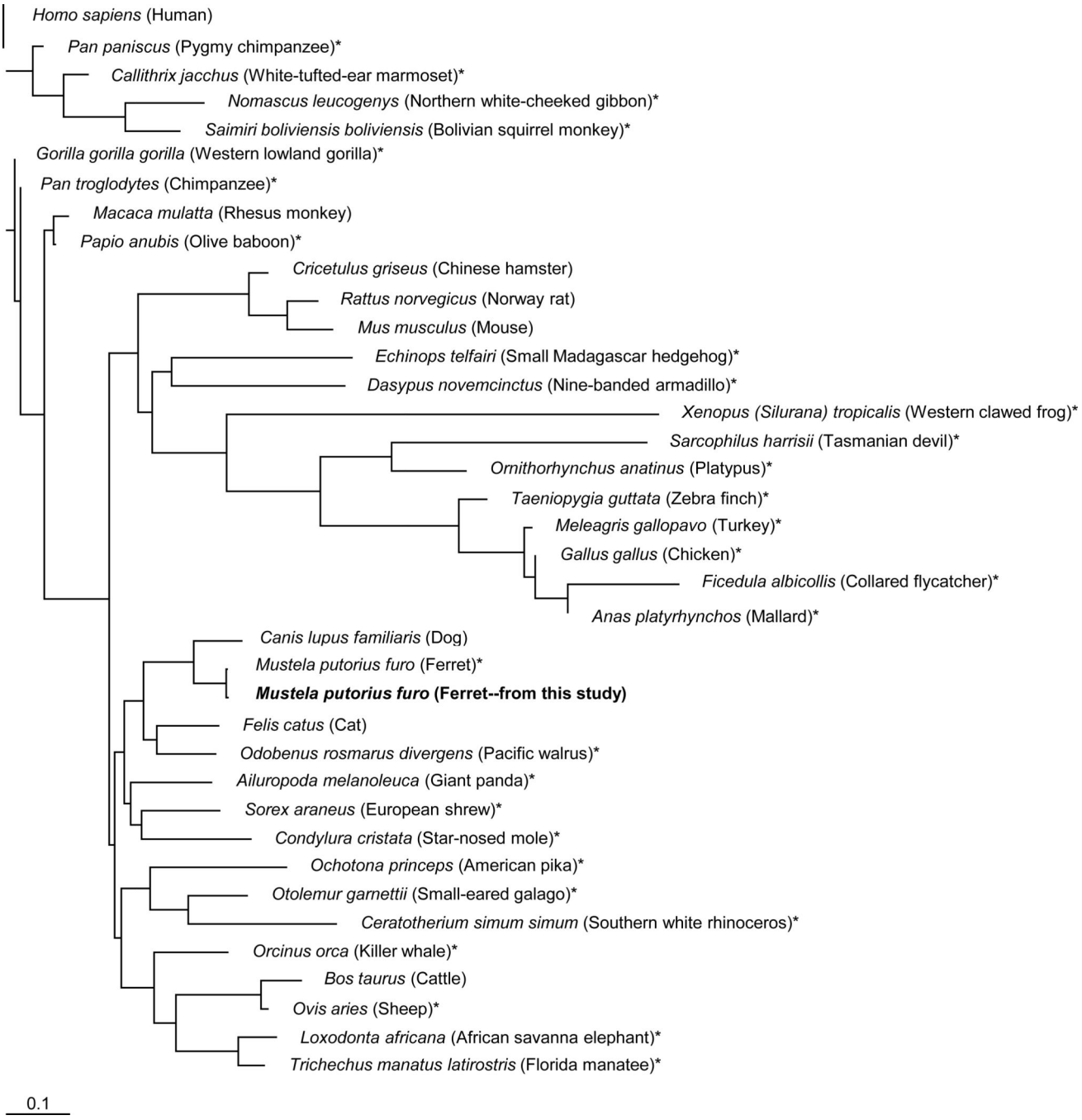

Fig. 1.

Phylogenetic analysis of the ferret podoplanin cDNA nucleotide sequence. The ferret podoplanin cDNA sequence obtained here was examined for its relatedness to podoplanin sequences from other species available from the NCBI/GenBank database. Predicted complete podoplanin ORF sequences derived from genomic DNA are indicated by (*). The phylogenetic tree was generated by the neighbor-joining method using the PHYLIP free program with 1000 bootstrap analyses and was drawn with Tree View 1.6.6 (Molecular Evolution).

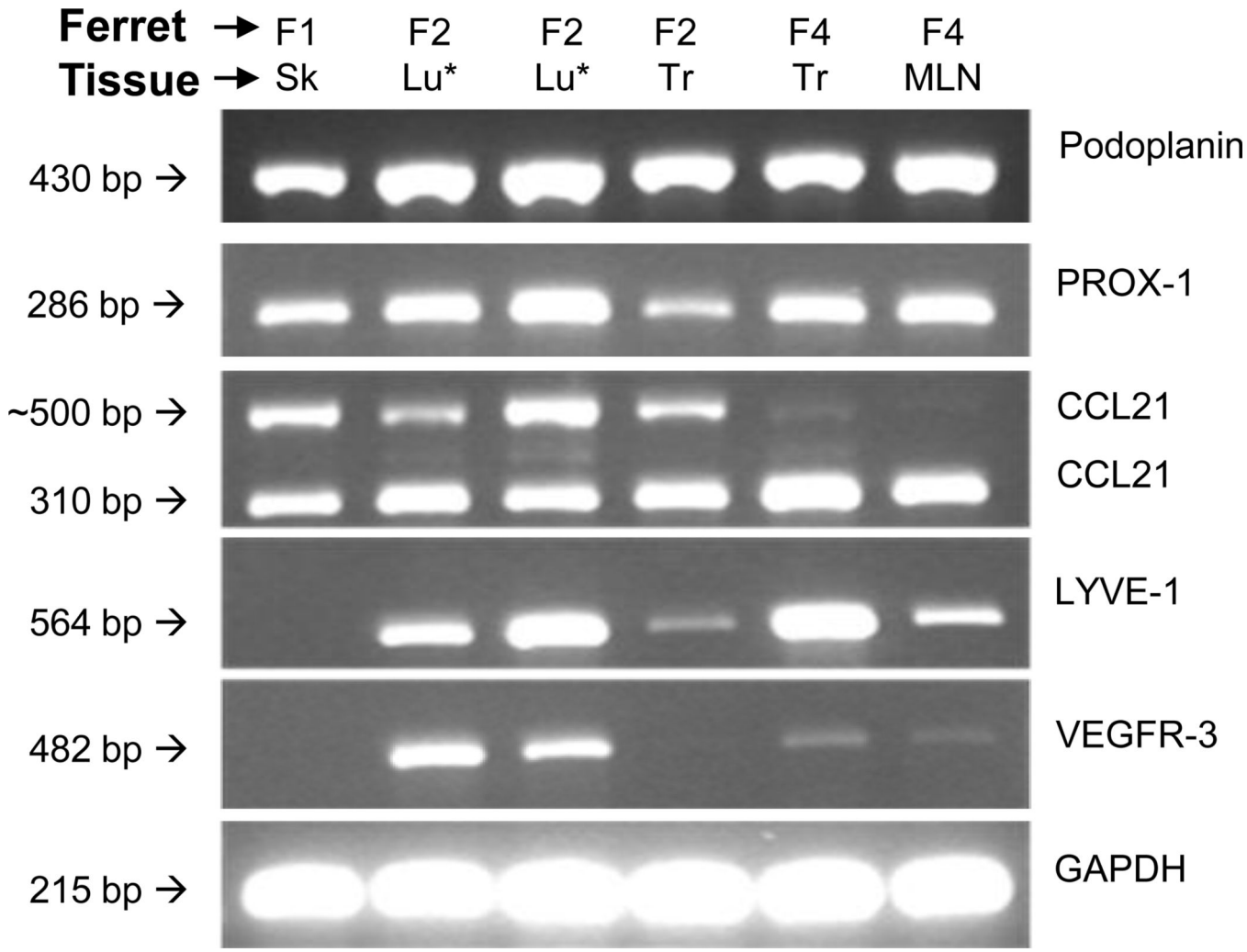

Fig. 2.

Ferret LECs express multiple LEC marker mRNAs. Standard RT-PCR was used to examine the expression of podoplanin, LYVE-1, PROX-1, VEGFR-3, and CCL21 in total RNA preparations from six ferret LEC populations. The ferrets and tissue types are noted above each column of bands, whereas the target gene is noted to the right of each gel image. The two lung LEC populations, noted by the asterisks (*), were derived from the left or right lobes of lung from the same animal.

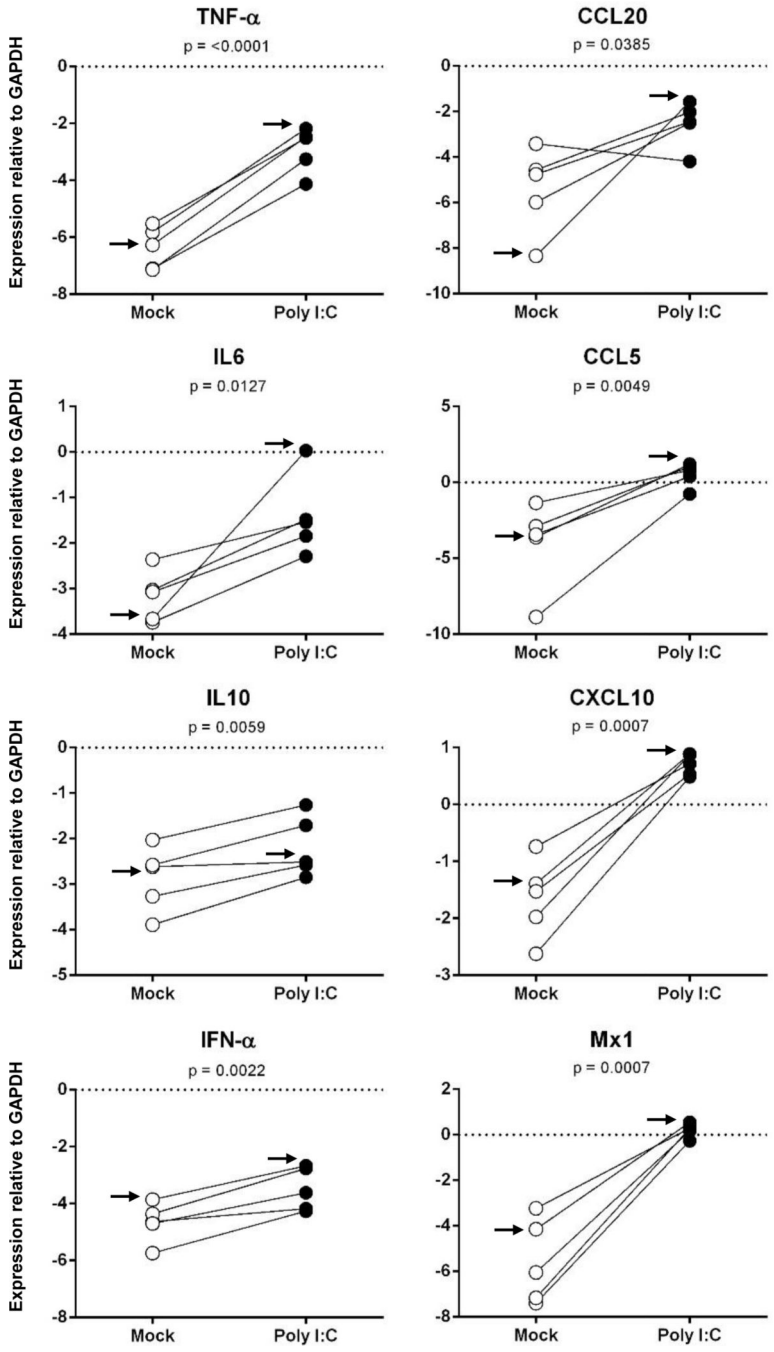

Fig. 3.

Primary ferret LECs respond strongly to poly I:C. Confluent monolayers of ferret skin (1 population), lung (1 population), trachea (2 populations), and mesenteric LN (1 population) LECs were exposed to poly I:C for 24 hours and responses were measured by SYBR Green real time RT-PCR for mRNAs encoding the indicated cytokine, chemokine, or ISG. Data are presented as values normalized to the endogenous control GAPDH calculated as $2^{(\Delta Ct)}$. The arrow denotes the data obtained from the lung LEC population used in Fig. 4.

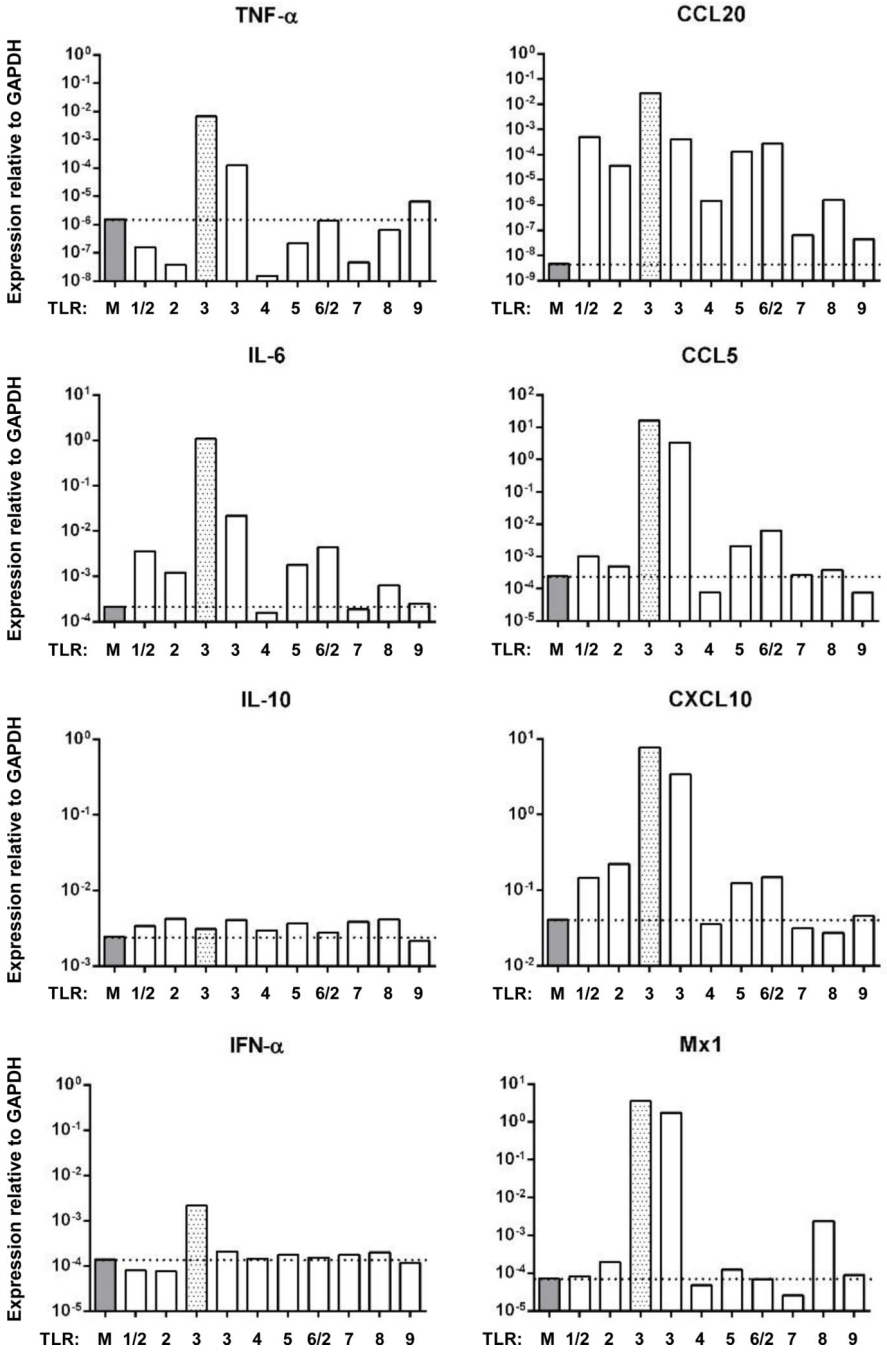

TLR	Ligand
M	Mock
1/2	Pam3CSK
2	HKLM
3	Poly I:C (HMW)
3	Poly I:C (LMW)
4	LPS
5	Flagellin
6/2	FSL-1
7	Imiquimod
8	ssRNA40
9	ODN2006

Fig. 4.

Ferret lung LEC responses to different TLR ligands. Ferret lung LECs (Ferret 2, left lobe lung LEC) were grown until 80 – 90% confluent and exposed to the indicated TLR ligands for 24 hr. The levels of the indicated mRNA targets were measured by real-time RT-PCR as presented in Fig. 3. The dashed line notes the level of expression of each mRNA in untreated cells. The grey bar denotes the poly I:C responses as a frame of reference for comparison to Fig. 3.

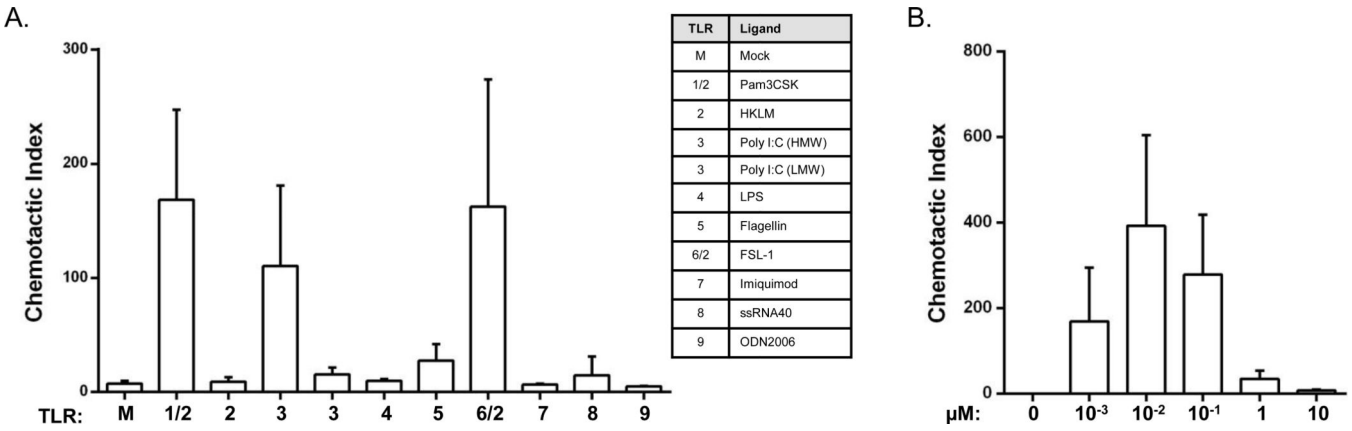

Fig. 5.

Chemotactic responses of ferret CCR6+ responder cells to LEC culture supernatants after TLR ligand stimulation. (A). Chemotaxis was performed using responder cells expressing ferret CCR6 and supernatants from control and TLR ligand treated ferret lung LECs. Chemotactic index (CI) was calculated relative to the medium only control (M). (B). Chemically synthesized ferret CCL20 (Qin et al., 2013) was used as a control (right). The data presented were combined from two independent experiments.

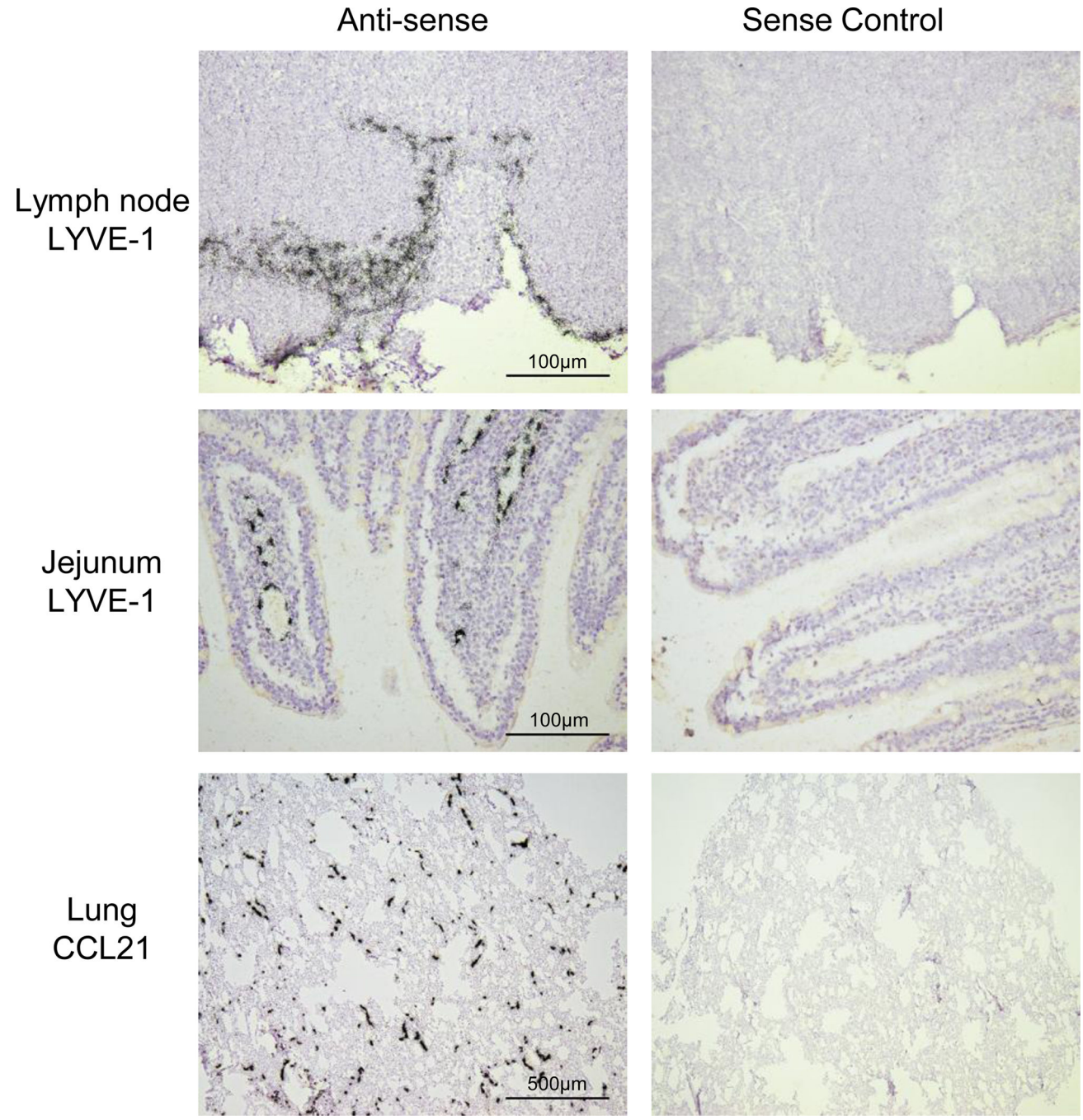

Fig. 6.

In situ hybridization localization of lymphatic marker mRNAs in ferret ferret lymph node, jejunal and lung tissues. ^{35}S-UTP-labeled riboprobes specific for ferret LYVE-1 or CCL21 were generated and used localize cells expressing the respective mRNAs in the indicated tissue from normal ferrets. ISH signal is visualized by collections black silver grains over cells. Parallel ISHs were performed with the cognate sense control probe (micrographs on the right). Exposure times were 21d.

Table 1

Nuceotide Sequence Relatedness of Ferret LEC Marker cDNAs to other animal species.

	Sequence identity (%)				
	Podoplanin (complete ORF)	**LYVE-1 (partial ORF)**	**PROX-1 (partial ORF)**	**VEGFR-3 (partial ORF)**	**CCL21 (complete ORF)**
Species					
Dog	81[a] (73)	91 (85)	98 (100)	92 (96)	89 (85)
Cat	82 (65)	90 (83)	98 (100)	94 (99)	90 (88)
Pig	71 (53)	80 (71)	98 (100)	92 (95)	84 (78)
Human	74 (60)	80 (65)	98 (100)	91 (94)	86 (80)
Rhesus	73 (59)	80 (67)	98 (100)	91 (95)	82 (77)
Mouse	78 (48)	76 (56)	95 (100)	87 (94)	80 (79)
Rat	80 (48)	76 (53)	95 (100)	86 (94)	76 (70)
Guinea pig	42 (37)	75 (63)	97 (99)	89 (94)	80 (76)
Syrian hamster	82 (46)	76 (60)	94 (99)	88 (96)	80 (71)

Data shown are the percent relatedness to the corresponding stretch of nucleotide sequences in the ferret cDNAs obtained here. The numbers in parentheses represent the percent relatedness of the corresponding deduced amino acid sequences.

Table 2

Primers and Sequences Used for Standard and Real-time RT-PCR.

RT-PCR	Primer name	Primer sequence (5'→3')	Amplicon size (bp)	Source
Standard	CaPDPNF1	AGATGTGGAGGGTGCCAGT	534	This study. Designed based on NM_001003220.
	CaPDPNR1	AATTCTTCAGCTCTTTAGGGCGAG		
Standard	CaLYVE-1F1	CTGGTGGTTGTCTGCTTCCAT	761	This study. Designed based on XM_003639783.
	CaLYVE-1R2	TGCAAAGAAGAGGAGTGCGAG		
Standard	CaProx-1F1	AATAGCCTCTAAACAGTTTC	382	This study. Designed based on XM_853042.
	CaProx-1R1	TATCCTCCTGATGTACTTCG		
Standard	CaVEGFR-3F3	GAGCTCTATGACATCCAGCTGT	537	This study. Designed based on XM_538585.
	CaVEGFR-3R3	GGCACATTCACCACCAGCTCCAG		
Standard	CaCCL21F1	TCCACCTCGCGCACTACTC	414	This study. Designed based on NM_001005258.
	CaCCL21R2	CTCTAGGCTGGTCACTGGG		
Standard	CaGAPDHF1	ATGGTGAAGGTCGGAGTCAA	300	This study. Designed based on NM_001003142.
	CaGAPDHR1	GAAGACCCCAGTGGACTCCA		
Standard	FePDPNF1	ATGTGGAGGGTGCCAGTTCT	430	This study. Designed based on obtained ferret sequence.
	FePDPNR1	CTGTCGCCAGACCATCTTTT		
Standard	FeLYVE1F1	GCCAAATGCTTCAGCCTGGT	564	This study. Designed based on obtained ferret sequence.
	FeLYVE1R1	AGCCCGAGCAGAAGTAGGAG		
Standard	FePROX-1F1	ATGCCTGACCATGACAGCAC	286	This study. Designed based on obtained ferret sequence.
	FePROX-1R1	GCTGGGAAATTATGGTTGCT		
Standard	FeVEGFR3F1	TGAGCTCTATGACATCCAGC	482	This study. Designed based on obtained ferret sequence.
	FeVEGFR3R1	CCTTTAGTACCAGGGCATGC		
Standard	FeCCL21F1	ATGGCTCAGTTACTGACTCC	310 (smaller fragment)	This study. Designed based on obtained ferret sequence.
	FeCCL21R1	TACAGCCCTGGACTTGTTTC	~500 (larger fragment)	
Standard	FeGAPDHF1	CATCGTGGAGGGCCTCATGA	215	This study. Designed based on obtained ferret sequence.
	FeGAPDHR1	ATACATTGGGGGTGGGGACAC		
Real time	SYBRfPDPNF1	GAGGATGGGCCAACTCAAGA	79	This study. Designed based on obtained ferret sequence.
	SYBEfPDPNR1	GTTGTGGTGCTCTGGCTTTCT		
Real time	SYBRfLYVE1F1	GCTTCAGCCTGGTGTTGCTT	79	This study. Designed based on obtained ferret sequence.
	SYBRfLYVE1R1	GATGTGACCAGGAGCCTTGTG		
Real time	SYBRfGAPDHF	TTGCTGACAATCTTGAGGGAGTT	81	This study. Designed based on obtained ferret sequence.
	SYBRfGAPDHR	CTGCTGATGCCCCCATGT		
Real time	SYBRfCCL20F	TGCTCCTGGCTACTTTGATGTC	89	This study. Designed based on published ferret CCL20 (Qin et al., 2013)
	SYBRfCCL20R	TGCTTGCTGCTTCTGACTTG		

Vet Immunol Immunopathol. Author manuscript; available in PMC 2016 February 15.

Table 3

Spearman's Correlation Analyses of mRNA Expression Levels in TLR Ligand Treated Ferret LECs.

	CCL5	CCL20	CXCL10	IFNα	IL6	IL10	Mx1	TNFα
CCL5	ID[a]	**0.95[b] (<0.0001)**	**0.76 (0.009)**	0.46 (0.155)	**0.93 (0.0001)**	0.36 (0.286)	0.56 (0.076)	0.37 (0.261)
CCL20		ID	**0.75 (0.011)**	0.37 (0.261)	**0.89 (0.0005)**	0.30 (0.371)	0.53 (0.100)	0.25 (0.468)
CXCL10			ID	0.12 (0.735)	**0.85 (0.0018)**	0.06 (0.860)	0.56 (0.082)	0.46 (0.173)
IFNα				ID	0.41 (0.2141)	0.21 (0.539)	0.45 (0.173)	0.51 (0.114)
IL6					ID	0.17 (0.615)	**0.67 (0.028)**	0.58 (0.066)
IL10						ID	0.41 (0.214)	−0.33 (0.327)
Mx1							ID	0.56 (0.076)
TNFα								ID

[a] ID, identical with r = 1.00.

[b] Shown are the r-values with the p-values presented in parentheses.